

Design improvement of permanent magnet flux switching motor with dual rotor structure

H. A. Soomro, E. Sulaiman, R. Kumar, N. S. Rahim

Research Centre for Applied Electromagnetics, Universiti Tun Hussein Onn Malaysia
Batu Pahat, 86400, Johor, Malaysia

Corresponding author: engg.hassansoomro@gmail.com, erwan@uthm.edu.my,
rajeshkumar@iiee.edu.pk,

Abstract. This paper presents design enhancement to reduce permanent magnet (PM) volume for 7S-6P-7S dual rotor permanent magnet flux-switching machines (DRPMFSM) for electric vehicle application. In recent years, Permanent magnet flux switching (PMFS) motor and a new member of brushless permanent magnet machine are prominently used for the electric vehicle. Though, more volume of Rare-Earth Permanent Magnet (REPM) is used to increase the cost and weight of these motors. Thus, to overcome the issue, new configuration of 7S-6P-7S dual rotor permanent magnet flux-switching machine (DRPMFSM) has been proposed and investigated in this paper. Initially proposed 7S-6P-7S DRPMFSM has been optimized using “deterministic optimization” to reduce the volume of PM and to attain optimum performances. In addition, the performances of initial and optimized DRPMFSM have been compared such that back-emf, cogging torque, average torque, torque and power vs speed performances, losses and efficiency have been analysed by 2D-finite element analysis (FEA) using the JMAG-Designer software ver. 14.1. Consequently, the final design 7S-6P-7S DRPMFSM has achieved the efficiency of 83.91% at reduced PM volume than initial design to confirm the better efficient motor for HEVs applications.

1. Introduction

The rise in the mean surface temperature on the earth has become an important issue in the 21st century which causes global warming. Scientists reported that the geomagnetic variation, the variations in the incoming solar radiation and the increasing greenhouse gasses by certain activities such as the burning of fossil fuels, deforestation etc are the foremost causes of global warming [1-2]. The vehicles with the conventional internal combustion engine (ICE) are likewise the leading sources of this issue. In response to worldwide temperature alteration issues, hybrid electric vehicles (HEVs) were the proposed solution to reduce the concentration of greenhouse gasses [3-4].

HEV has two power sources, one bidirectional power source based on electrical energy storage subsystem with an electric machine and the other unidirectional power source based on ICE [5]. Any electric machine, DC or AC, is considered as a physical device to succeed electromechanical energy conversion. The basic provisions of an electric machine for electric vehicle drive system are high efficiency, high torque density, and constant power at high speed [6]. For HEVs, DC motors are used widely due to their advantage of simple control of the orthogonal disposition of field and armature mmf. However, the maintenance problem of commutators and brushes makes them less reliable and unsuitable for HEV applications [7].



Meanwhile, switch reluctance machine (SRM) and induction machine (IM) have been perceived to have an impressive potential for HEVs due to their low cost and low maintenance. The presence of breakdown torque of an induction motor limits the extended constant-power operation. If the IM is operated beyond the critical speed which is two times the synchronous one, it will halt the motor. Although SRMs have the simple construction and low cost but they usually exhibit acoustic-noise problems. In addition, it is difficult to control the speed of SRM. One example of a successfully developed machine for HEVs is an interior permanent magnet synchronous machine (IPMSM). IPMSM consists of a large volume of the permanent magnet located in the rotor as their main flux sources. Though IPMSMs have achieved high torque and power density but the mechanical strength of rotor reduced and cost of machine increased due to high volume PM in the rotor [8-9].

In order to develop an appropriate machine for HEVs a new type of electric motor was discovered in [10] known as flux switching motor (FSM) with advantages of higher torque density, and efficiency. FSM resides all active parts on stator side with robust rotor structure without winding to overcome temperature rise. Furthermore, FSMs are classified into three types with respect to their field excitation sources such as permanent magnet (PM) FSM, field excitation (FE) FSM and hybrid excitation flux (HE) FSM [11-12].

Moreover, the PMFSM has become progressively prevalent in recent years for various industrial and HEVs applications. A PMFSM, which embodies the combined merits of permanent magnet synchronous machines (PMSMs) and switching reluctance machines (SRMs), offers several desirable features such as high torque and power density, the robustness of rotors and a significant degree of fault tolerant capabilities [13].

Although most of the reported PMFSMs can obtain relatively high torque and power density, they also suffer from high cogging torque and torque ripple due to their doubly salient structure and high airgap flux density caused by flux focusing effects. It is imperative to minimize such torque pulsations in HEVs applications to avoid undesirable vibration and acoustic noise and to provide accurate position and speed control [14]. Although traditional approaches, such as skewing, tooth and magnet shaping, or drive control methods, can be adopted to reduce cogging torque and torque ripple, these approaches certainly introduce performance degradation and increase manufacturing difficulties. Furthermore, the fault-tolerant capabilities of PMFSMs are essential to be further improved to spread them for HEVs applications [15].

Therefore in this paper, a new 7S-6P-7S dual-rotor (DR) PMFSM is proposed and optimized for HEVs applications, in which the phase group concentrated-coil windings and unaligned arrangement of the two rotors are utilized. The unaligned arrangement of the two rotors will help to achieve increased flux amplification and also to suppress the cogging torque and torque ripples. Initially, a new structure of 7S-6P-7S dual-rotor DRPMFSM is designed using 2D finite element analysis (FEA). Subsequently, initial design has been optimized to fulfill the optimum performance requirement for HEVs. The significant of optimization is to reduce the volume of rare earth magnet as it is costly.

2. Design restriction and specification with geometric topology

Figure 1 shows the initial design of proposed 7S-6P-7S DRPMFSM, which contains dual rotors. The inner and outer rotor which are the moving parts of the motor whereas the stator, PM and armature coil winding are the static parts. Design specifications are tabulated in Table 1. From table 1, it is observable that radii of the outer rotor and inner rotor are 45mm and 18.6mm respectively with stator radius of 35.4mm. The air gap between both the rotors and stator has been set at 0.6mm for better flux linkage from the stator to rotors. Furthermore, the corresponding electrical restrictions to the inverter such as maximum DC bus voltage and maximum inverter current are set to 415V and 360Arms, respectively, while the maximum armature current density J_a has been set to 30Arms/mm². The volume of PM used is 244.8g which is located in between armature slots.

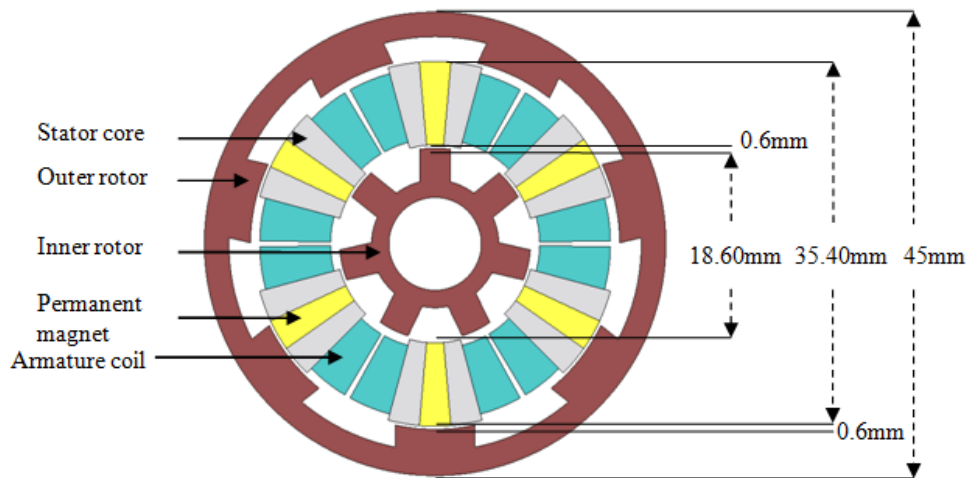


Figure 1. 2D initial design of the DRPMFSM

Table 1. Design restrictions and specifications of initial		
Restriction and specification	Description	7p-6s-7p DRPMFSM Initial
Geometric & Motor Spec.	PM weight (g)	244.8
	Motor stack length (mm)	70
	Outer rotor radius (mm)	45
	Outer rotor pole height(mm)	7.8
	Inner rotor radius (mm)	18.6
	Inner rotor pole height	3
	Stator radius (mm)	35.4
	Permanent magnet height	16.2
	Armature coil slot height	15
	Shaft radius (mm)	9
	Outer and inner rotor air gap (mm)	0.6
	Max. current density in armature coil, J_a (Arms/mm ²)	30

3. Machine optimization approach

The optimization process is focused on improving the initial design of 7P-6S-7P DRPMFSM till the target performances achieved as shown in Figure2. Additionally, the main intention is to reduce the PM volume with similar target magnitudes. To enhance the target performances “deterministic optimization” approach has been used by changing the defined parameters of motor parts such as the radius of the outer and inner rotor, stator radius, armature slot dimensions, PM dimensions and number of turns. Whereas during varying the dimension of any motor part the rest dimensions must be taken constant until optimum average torque attained. Similarly, this technique is repeated for all other parameters. The detailed parameters from D1 to D2 are shown in Figure3, which are optimized. After successful accomplishment of the optimization process of initial design considering initial performances, the final parameters of final design are tabulated in Table 2. From the table, it is obvious that almost all parameter dimensions are changed with PM. It is also notable from the table

that almost 40% volume of PM has been reduced after optimization. Figure 4 shows the design of initial and final optimized 7P-6S-7P DRPMFSM in which PM volume reduction can be notified.

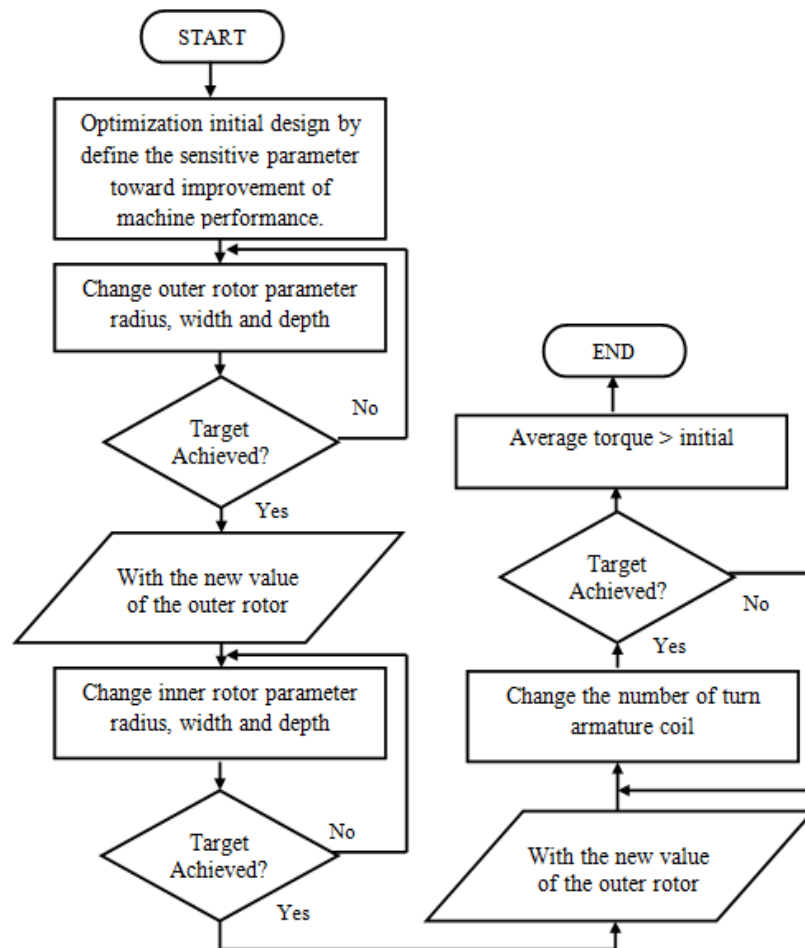


Figure 2. Workflow of general for optimization

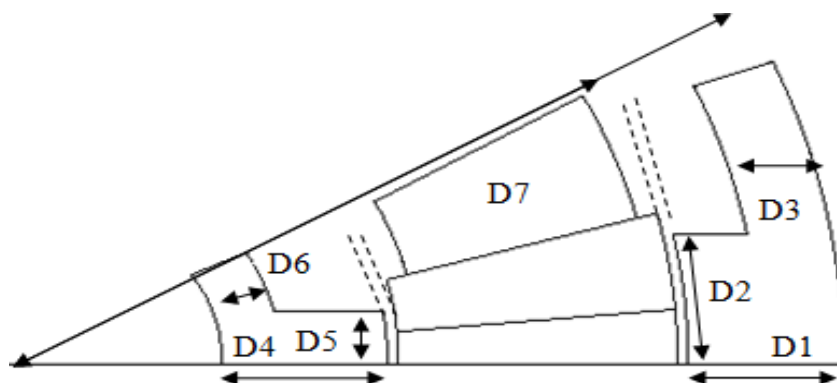


Figure 3. Different Parameter form D1 to D7

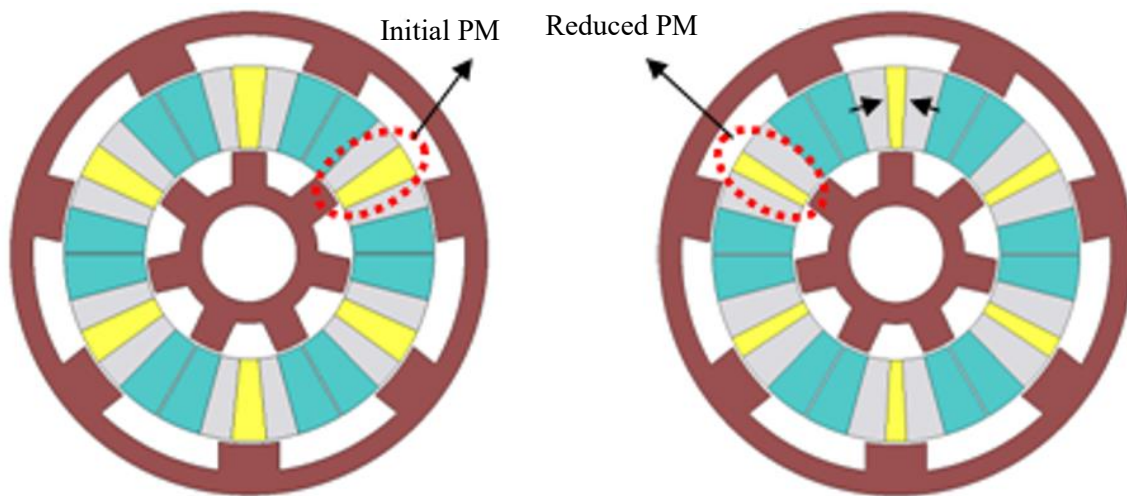


Figure 4. Initial and final optimized design of DRPMFSM

Table 2. Initial and Final optimized design specifications

Description/Item		Initial design	Final design >PM	Unit
Outer rotor	Radius (inner)	36	35.50	mm
	Pole width	7.80	5.80	mm
	Pole depth (yoke)	4.80	4.25	mm
Inner rotor	Radius (outer)	18.60	19.10	mm
	Pole width	3	3.25	mm
	Pole depth (yoke)	3.4	4.0	mm
Slot area of armature coil, S _a		92.07	101.55	mm
Motor stack length (mm)		70	70	mm
Permanent magnet	Length	16.20	15.2	mm
	Width a	1.67	1.10	mm
	Width b	3.09	1.95	mm
Shaft radius		9	9	mm
Outer rotor air gap		0.6	0.6	mm
Inner rotor air gap				mm
Stator	Length	16.20	15.20	mm
	Width a	3.35	4.26	mm
	Width b	6.17	7.54	mm
Number of armature coil turn		188	200	mm

4. Result and Performance

The performances of the initial and optimized 7S-6P-7S DRPMFSM has been analysed by 2D FEA using JMAG software. Firstly flux distribution, back emf, and cogging torque have been analysed at open circuit conditions, secondly, torque and power vs speed, losses and efficiency analysis have been conducted at short circuit conditions. Afterward, all results of initial and optimized 7S-6P-7S DRPMFSM have been compared to adopt the appropriate design for HEVs applications.

4.1. Back emf of initial and optimized 7S-6P-7SDRPMFSM

Back emf of initial and optimized 7S-6P-7SDRPMFSM have been conducted at open circuit condition or no load condition where armature current, $I_a=0$, the induced voltage generated from PM at the speed of 500 revs/min is illustrated in Figure 5. It is obvious from the figure that voltage generated from initial design and optimized design are 264.06V and 272.58V respectively. Though the final design has 2.23% more voltage induction than initial. However, the voltage supply is set to 415V, the induce voltages of initial and final designs are less than that amount hence motors will work on safe regions. Besides back emf achieved by both designs is sinusoidal waveform and produce less distortion. These less value of back-emf gives the advantage of easy protection when the inverter is in off state due to uncertain faults.

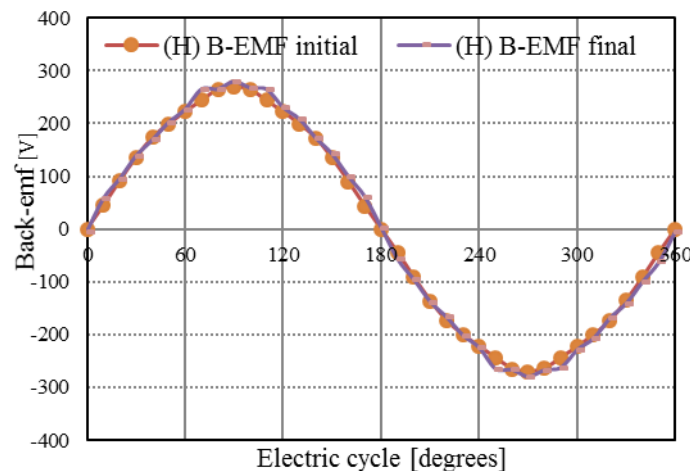


Figure 5. Back EMF for the initial and final optimization design DRPMFSM

4.2. Cogging torque of initial and optimized 7S-6P-7S DRPMFSM

The cogging torque analysis initial and optimized 7S-6P-7SDRPMFSM examined by setting armature current density, $J_a=0$ as illustrated in Figure 6. It is apparent from the Figure that the cogging torque of optimized design consists of six cycles at maximum peak-to-peak of values of approximately 1.104Nm making rotor in synchronizing rotation. This value is considered low with respect to the output torque. The value of cogging for the optimized design is greater than the initial design, yet it's in the low range as peak to peak value of cogging torque should be below 10% of average torque.

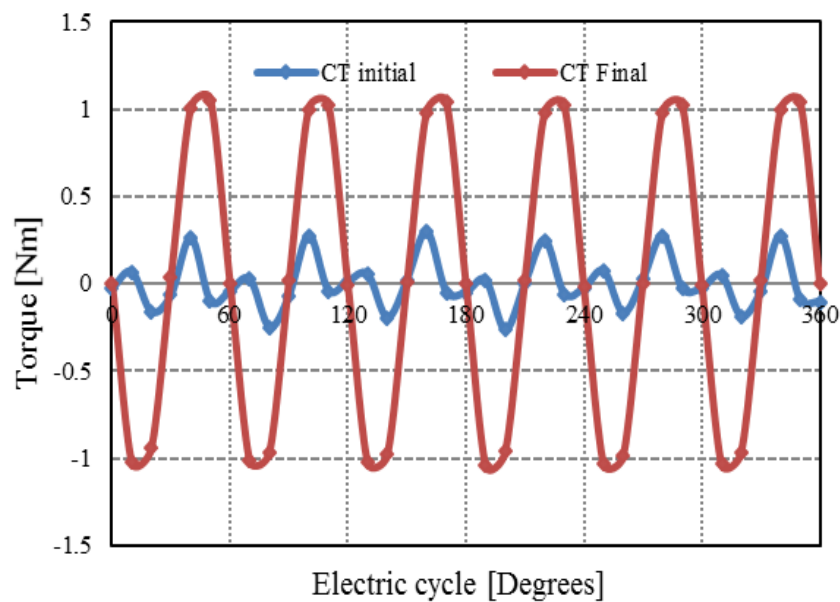


Figure 6. Cogging torque for initial and final optimization of the DRPMFSM

4.3. Torque performances at load conditions

The examination of torque performances has been carried out at maximum armature current density, $J_a=30$ Arms/mm² for both the initial and optimized design of DRPMFSM. Figure 7 depicts the performances of output torque for both designs. From the figure, it is obvious that final optimized design has attained slightly increment in torque performance than initial that 2.23% at maximum armature current density. At the initial stage, although the torque increased is less but still, the machine is appropriate for HEVs as the torque generated by final design is approximately 18Nm. However, by further design refinement and enhancement, the torque performances are expected to reach the highest values.

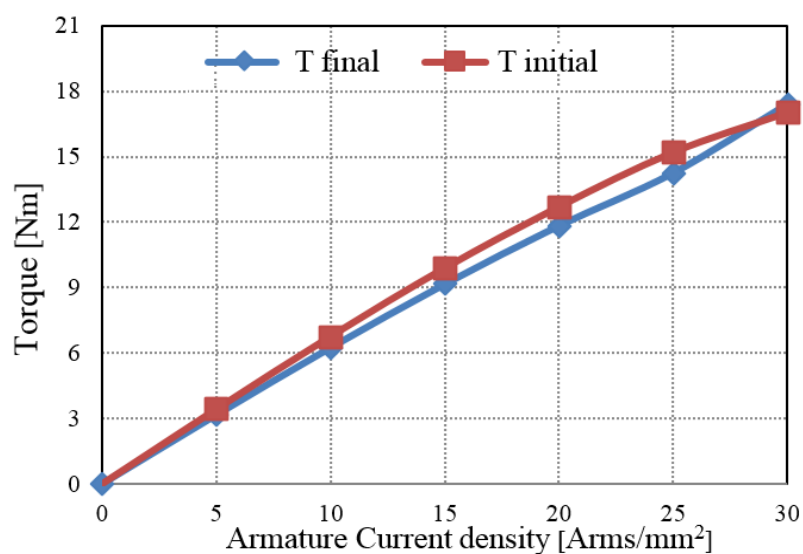


Figure 7. Torque of the initial and final optimization of DRPMFSM

4.4. Torque and power vs speed characteristics

The torque and power versus speed curves of initial and final optimized designs of 7S-6P-7S DRPMFSM are plotted in Figure 8. At the base speed of approximately 500rev/min and 700 revs/min, the maximum torque of approximately 17.5 Nm and 17 Nm is obtained for final and initial designs respectively and torque starts to decrease if the machine is operated beyond the base speed. The power accomplished by initial design of 7S-6P-7S DRPMFSM at base speed of 2200 rev/min is around 1249W and starts to reduce until 1173.9W at higher speed of 6080.85 rev/min due to increase in iron loss while the power attained by final optimized design is 1600W at maximum torque at base speed of 2020.67 revs/min which is 26.6% more than the initial DRPMFSM.

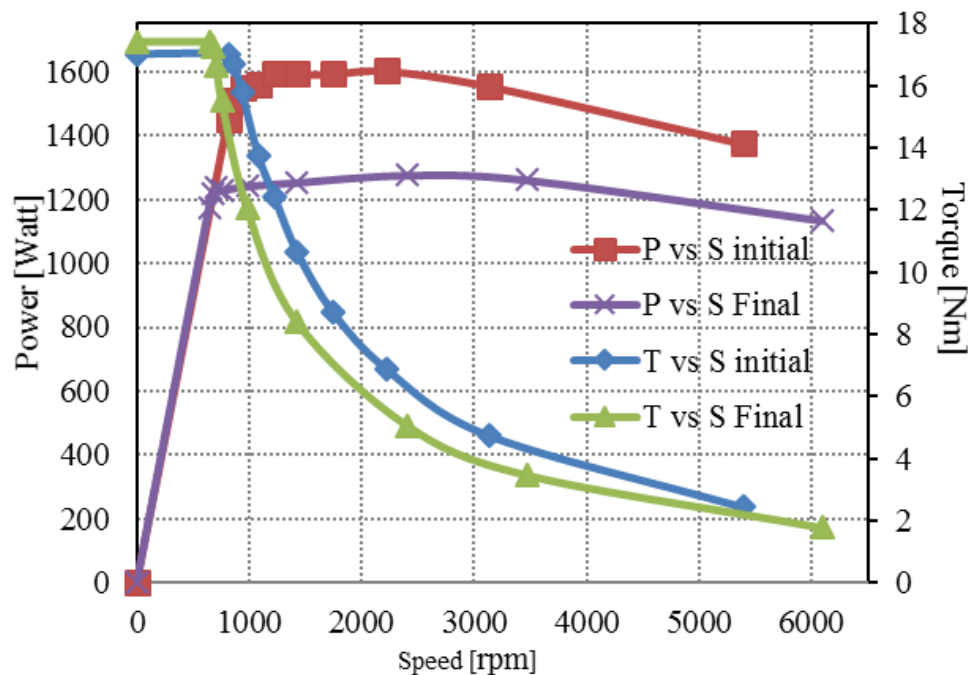


Figure 8. Torque and power vs speed characteristics of initial and final design of DRPMFSM

4.5. Motor loss and efficiency analysis

The motor losses and efficiency are calculated using 2FEA, taking into consideration the copper losses in armature coil and the iron loss in all laminated cores of the stator and rotor. The motor losses and efficiency at the specific operating point such that at starting speed, at high speed, and at frequent operating conditions are defined by point No. 1 to No. 8 as shown in Figure 9. The Figure shows the point No. 1 with the base speed of 814.47rpm at 17.02 Nm for the initial design and 644.13rpm at 17.40Nm for the final design. Point No. 2 is the maximum speed with 3128.14rpm at 4.75Nm for the initial design and 3466.97rpm at 3.472Nm for the final design. While point No. 3, 4, 5, 6, 7 and 8 are frequent speed from 500rpm until 1500rpm for both designs. Based on all these points, iron losses (P_i) and copper losses (P_c) are analysed to calculate the efficiency of the motor.

Furthermore, Figure 10 and 11 illustrates the comparison of initial design and final optimized design of iron losses (P_i) and copper losses (P_c) respectively. From Figure 10, at point No. 2 iron losses of final design are around 30% higher than initial design due to the reason that final design goes for higher speed ranges as compared to initial design. On the other hand at normal operating points, the final design has fewer iron losses as compared to initial design. From the observation on Fig. 11, at point No. 1 the copper losses are higher for both designs than the other operating points due to the reason that at point No. 1 maximum armature current has been injected and more current has been

drawn. Copper losses at starting point are 847.1W and 959.92W for initial and final optimized design respectively.

Additionally, Figure 12 shows the efficiency comparison of the initial and final design with reduction of PM volume on the eight operating points. The average efficiency of the initial and optimized DRPMFSM are 83.5% and 83.91% respectively. Thus, the efficiencies of both designs are almost same and are appropriate to be used for HEVs applications.

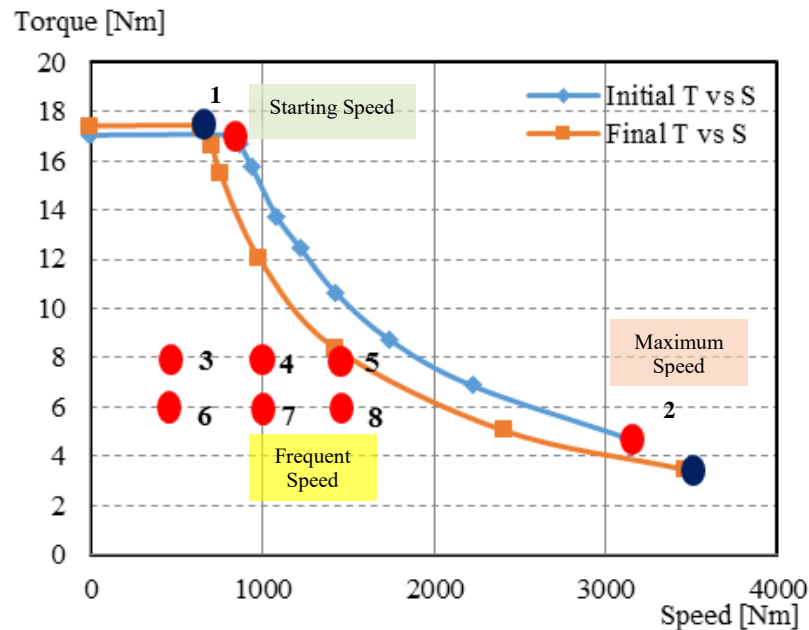


Figure 9. Torque vs speed curve of the initial and final design DRPMFSM for locating operating points

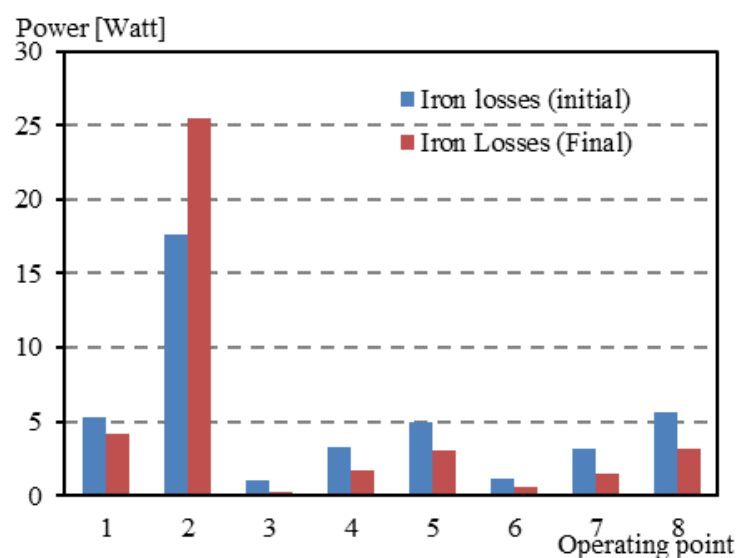


Figure 10. Comparison of the power iron losses of the initial and final design of DRPMFSM

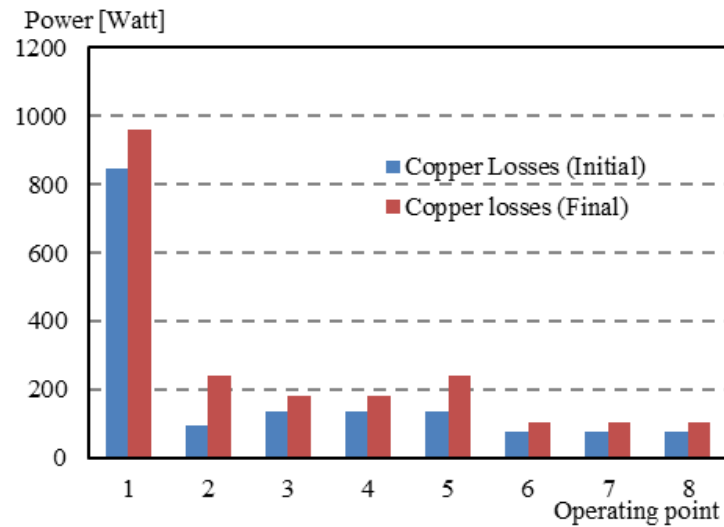


Figure 11. Comparison of the power iron losses of the initial and final design of DRPMFSM

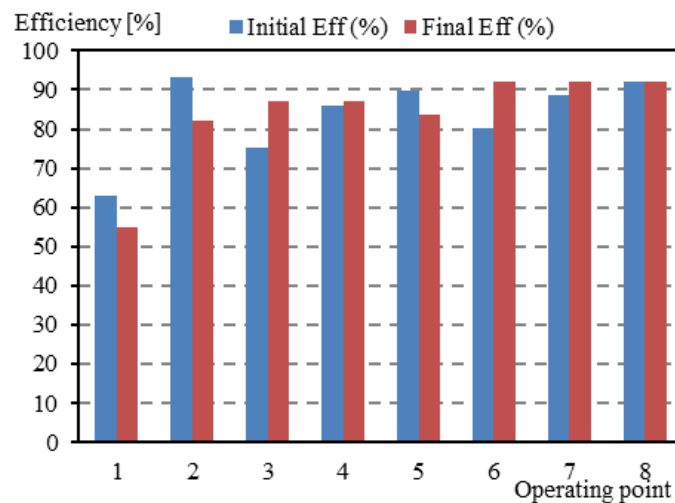


Figure 12. Comparison of the efficiency of the initial and final design of DRPMFSM

5. Conclusion

In this paper, a design improvement of 7S-6P-7S DRPMFSM has been analysed. This paper is focused on the deterministic optimization to increasing the torque performances with less PM volume. Consequently, after using optimization techniques 40% volume of PM has been reduced, which decreases the cost of the motor with similar torque performances as initial design.

In addition, comparison analysis of initial and final optimized designs have been executed, such that cogging torque, back emf, analysis of torque and power with speed and efficiency. Subsequently, it has been found that both the initial and optimized designs of 7S-6P-7S DRPMFSM are suitable for

HEVs applications. Although optimized 7S-6P-7S DRPMFSM has attained higher performances at less cost as compared to initial design.

References

- [1] Samuel S, Sivamadhavi V 2010 *Recent Advance in Space Technology Services and Climate Change (RSTSCC)* p 41.
- [2] Ahmad M. Z, Sulaiman E and Haron Z.A 2013 *Dept.of Electric Power Engineering University Tun Hussein On Malaysia johor, IEEE 7th Int. Power Eng. and Opt. Conf. (PEOCO)* p 298.
- [3] Md Zafari Ahmad, Erwan Sulaiman, Zainal Alam Haron 2014 *applied mechanics and materials, Trans Tech. Publications, Switzeland* , **9** 787.
- [4] Mahyuzie J, Sulaiman E, Mohd F. O, Gadafi M. R, Soomro. H. A 2015 *IEEE Student Conference on Research and Development (SCORED)* p 298.
- [5] Gerfried C IEEE International Conference on Connected Vehicles and Expo (ICCVE) p. 713
- [6] Emadi A, Young J. L, Rajashekara K 2008 *IEEE Trans. Ind. Electron* **55** p 2237
- [7] Khan F, Sulaiman E, Ahmad M.Z, Ali H 2014 *International Conference on Frontiers of Information Technology (FIT)* p 298.
- [8] Sulaiman E, Kosaka T, and Matsui N 2014 *Renewable and Sustainable Energy Review* **34** p 517.
- [9] Ruiwu C, Chris M, Fellow, IEEE, and Ming C 2012 *IEEE Transactions on Magnetics* **48** p 2374
- [10] Sulaiman E , Aminl N. S. M, Husin Z. A, Ahmad M. Z and Kosaka T 2013 *IEEE 7th International Power Engineering and Optimization Conference (PEOCO)* p 40
- [11] Kumar R, Sulaiman E, M Jenal M, Jusoh L. I, Bahrim F. S 2016 *International Journal of Power Electronics and Drive Systems (IJPEDS)* **8**
- [12] Sulaiman E, Kosaka T, and Matsui N 2011 *IEEE Transactions on Magnetics* **47** p 4453.
- [13] Zulu A, Mecrow B. C, and Armstrong M, 2012 *IEEE Transactions on Industry Applications* **48** p. 2259.
- [14] Fei W, Luk P. C. K, and Shen J. X, 2012 *IEEE Transactions on Magnetics* **48**, p 2664
- [15] Zhao W, Lipo T A, Life Fellow IEEE and Kwon B Senior Member IEEE 2015 *IEEE Transactions on Magnetics* **51**